Lifetime of Anthropogenic Climate Change: Millennial Time Scales of Potential CO_2 and Surface Temperature Perturbations

M. EBY, K. ZICKFELD, AND A. MONTENEGRO

School of Earth and Ocean Sciences, University of Victoria, Victoria, British Columbia, Canada

D. ARCHER

Department of the Geophysical Sciences, University of Chicago, Chicago, Illinois

K. J. MEISSNER AND A. J. WEAVER

School of Earth and Ocean Sciences, University of Victoria, Victoria, British Columbia, Canada

(Manuscript received 2 April 2008, in final form 15 September 2008)

ABSTRACT

Multimillennial simulations with a fully coupled climate–carbon cycle model are examined to assess the persistence of the climatic impacts of anthropogenic CO_2 emissions. It is found that the time required to absorb anthropogenic CO_2 strongly depends on the total amount of emissions; for emissions similar to known fossil fuel reserves, the time to absorb 50% of the CO_2 is more than 2000 yr. The long-term climate response appears to be independent of the rate at which CO_2 is emitted over the next few centuries. Results further suggest that the lifetime of the surface air temperature anomaly might be as much as 60% longer than the lifetime of anthropogenic CO_2 and that two-thirds of the maximum temperature anomaly will persist for longer than 10 000 yr. This suggests that the consequences of anthropogenic CO_2 emissions will persist for many millennia.

1. Introduction

The projection of the climatic consequences of anthropogenic CO_2 emissions for the twenty-first century has been a major topic of climate research. Nevertheless, the long-term consequences of anthropogenic CO_2 remain highly uncertain. The Intergovernmental Panel on Climate Change (IPCC) Fourth Assessment Report (AR4) reported that ''about 50% of a CO_2 increase will be removed from the atmosphere within 30 years and a further 30% will be removed within a few centuries'' (Denman et al. 2007, p. 501). Although the IPCC estimate of the time to absorb 50% of CO_2 is accurate for relatively small amounts of emissions at the present time, this may be a considerable underestimation for large quantities of emissions. Carbon sinks may become saturated in the future, reducing the system's ability to absorb CO_2.

Atmospheric CO_2 is currently the dominant anthropogenic greenhouse gas implicated in global warming (Forster et al. 2007); therefore, estimating the lifetime of anthropogenic climate change will largely depend on the perturbation lifetime of CO_2. The perturbation lifetime is a measure of the time over which anomalous levels of CO_2 or temperature remain in the atmosphere (defined here to be the time required for a fractional reduction to $1/e$). Carbon emissions can be taken up rapidly by the land, through changes in soil and vegetation carbon, and by dissolution in the surface ocean. Ocean uptake slows as the surface waters equilibrate with the atmosphere and continued uptake depends on the rate of carbon transport to the deep ocean. Ocean uptake is enhanced through dissolution of existing $CaCO_3$, often referred to as carbonate compensation. As CO_2 is taken up, the ocean becomes more acidic, eventually releasing $CaCO_3$ from deep sediments. This increases the ocean alkalinity, allowing the ocean to take up additional CO_2. Carbonate compensation becomes important on millennial time scales, whereas changes in the weathering of continental carbonate and

Corresponding author address: M. Eby, School of Earth and Ocean Sciences, University of Victoria, P.O. Box 3055, Victoria, BC V8W 3P6, Canada.
E-mail: eby@uvic.ca

DOI: 10.1175/2008JCLI2554.1

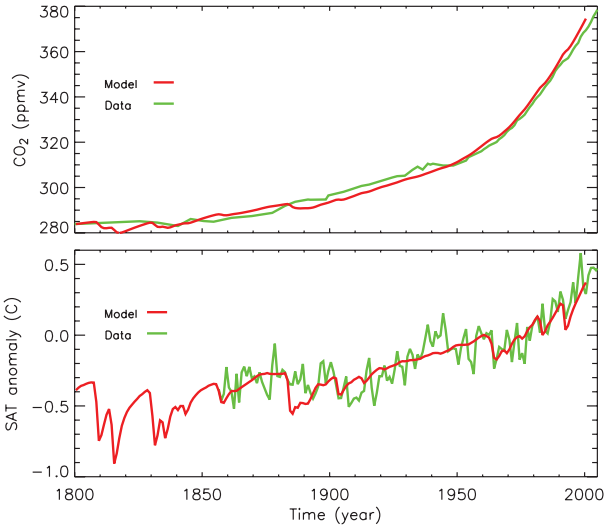

FIG. 1. Historical changes in CO_2 and SAT. (top) Model simulated CO_2 and (bottom) SAT are compared to historical data (Ethridge et al. 1998; Keeling and Whorf 2005; Jones et al. 2008). The model simulation includes all historical forcings (CO_2 emissions, insolation, orbital forcing, tropospheric and stratospheric sulfates and non-CO_2 greenhouse gases such as CH_4, N_2O, and CFCs).

silicate are thought to become important on the 10 000–100 000-yr time scale (Archer 2005; Sarmiento and Gruber 2006; Lenton and Britton 2006).

Earth system models can be used to simulate the evolution of the climate system under different anthropogenic emissions scenarios. There is still a great deal of uncertainty in the climate–carbon cycle response and considerable variation in model predictions. The short term (century time scale) may be dominated by the terrestrial carbon cycle response, which is poorly understood. Over the longer term (millennial time scale) the ocean biology, sediment, and weathering responses are also highly uncertain. Comprehensive model simulations of the next few centuries suggest that CO_2 anomalies may be relatively long lived (Friedlingstein et al. 2006; Plattner et al. 2008). These studies also illustrate the large uncertainties in the modeled short-term carbon cycle response but they were not designed to estimate the multimillennial response or the dependency of the recovery time scales on the level of emissions.

There are few modeling studies that have considered the coupled climate–carbon cycle response to large anthropogenic emissions on the 10 000-yr time scale. Differing levels of complexity and experimental design make a detailed comparison of other studies difficult, but most studies suggest that the average perturbation lifetime of most of the CO_2 is on the order of a few centuries and that as much as a quarter of the perturbation lasts for more than 5000 yr (Archer et al. 1998; Archer 2005; Archer and Brovkin 2008; Lenton and Britton 2006; Lenton et al. 2006; Ridgwell and Hargreaves 2007; Ridgwell et al. 2007; Mikolajewicz et al. 2007; Tyrell et al. 2007; Montenegro et al. 2007). None of these studies attempted to estimate the millennial time scales of the temperature response or investigated the multimillennial response as a function of the magnitude of the perturbation in a systematic way.

TABLE 1. Simulated global carbon inventories in 1800 and 1994 and their differences (in PgC). The estimated values are taken from the IPCC Fourth Assessment Report (Denman et al. 2007, Fig 7.3).

Year	Atmosphere	Vegetation + Soil	Ocean	Sediment
1800	591	604 + 1366 = 1970	37 237	1166
1994	761	661 + 1437 = 2098	37 340	1166
Difference	170	57 + 71 = 128	103	0
Estimate	165	101	118	0

Models that have looked at the long-term carbon cycle response are usually low resolution, highly parameterized, or incomplete. For example, Archer (2005) used highly parameterized climate feedbacks, whereas Montenegro et al. (2007) used two incomplete models: one model lacked a terrestrial carbon cycle and the other lacked ocean sediments. The model used here is currently one of the more complex coupled climate–carbon cycle models capable of looking at multimillennial time scales. Even given the large range in existing model predictions, we will show that the lifetime of both the anthropogenic CO_2 perturbation and the resulting surface air temperature (SAT) change may be longer than previously thought.

2. Model description and evaluation

We use version 2.8 of the University of Victoria (UVic) Earth System Climate Model (ESCM). It consists of a primitive equation 3D ocean general circulation model with isopycnal mixing and a Gent and McWilliams (1990) parameterization of the effect of eddy-induced tracer transport. For diapycnal mixing, a horizontally constant profile of diffusivity is applied, with values of about $0.3\ 10^{-4}\ m^2\ s^{-1}$ in the pycnocline. The ocean model is coupled to a dynamic–thermodynamic sea ice model and an energy–moisture balance model of the atmosphere with dynamical feedbacks (Weaver et al. 2001). The land surface and terrestrial vegetation components are represented by a simplified version of the Hadley Centre Met Office surface exchange scheme (MOSES) coupled to the Top-down Representation of Interactive Foliage and Flora Including Dynamic vegetation model; Meissner

TABLE 2. Modeled and estimated global carbon budgets are for the 1980s, 1990s, and 2000–05 in PgC yr^{-1}. The estimated values are taken from the IPCC Fourth Assessment Report (Denman et al. 2007, Table 7.1).

	1980s		1990s		2000–05	
	Model	Estimate	Model	Estimate	Model	Estimate
Atmospheric increase	3.3	3.3 ± 0.1	3.7	3.2 ±0.1	4.2	4.1 ± 0.1
Ocean uptake	−1.8	−1.8 ± 0.8	−2.2	−2.2 ± 0.4	−2.4	−2.2 ± 0.5
Land uptake	−2.2	−1.7 (−3.4 to 0.2)	−2.6	−2.6 (−4.3 to −0.9)	−2.8	n/a

et al. 2003). Land carbon fluxes are calculated within MOSES and are allocated to vegetation and soil carbon pools (Matthews et al. 2004). Ocean carbon is simulated by means of an Ocean Carbon-Cycle Model Intercomparison Project type inorganic carbon cycle model and a nutrient–phytoplankton–zooplankton–detritus marine ecosystem model (Schmittner et al. 2008). Sediment processes are represented using an oxic-only model of sediment respiration (Archer 1996a).

An earlier version of the UVic ESCM (version 2.7) has undergone extensive evaluation as part of international model intercomparison projects including the Coupled Carbon Cycle Climate Model Intercomparison Project (Friedlingstein et al. 2006), the Paleoclimate Modeling Intercomparison Project (Weber et al. 2007), and the coordinated thermohaline circulation experiments (Gregory et al. 2005; Stouffer et al. 2006). The model has also been used for multicentury climate projections in support of the IPCC Fourth Assessment Report (Denman et al. 2007; Meehl et al. 2007). Here, we evaluate the UVic ESCM version 2.8 primarily with respect to its ability to simulate characteristics of the coupled climate–carbon cycle system, including the air–sea flux of CO_2, the distribution of ocean dissolved inorganic carbon (DIC) and alkalinity, the percent of $CaCO_3$ in sediments, the global carbon budgets of the last decades and the observation-based evolution of surface air temperature and CO_2 over the historical period. From a preindustrial climate, this version of the model has a transient climate response of 2.0°C and an equilibrium climate sensitivity of 3.5°C (Weaver et al. 2007).

The simulated evolution of atmospheric CO_2 and surface air temperature over the historical period is in good agreement with observations (Fig. 1). For the year 2000, the simulated CO_2 is about 5 ppmv higher than the observation-based value. The model does not produce as much interannual variability as seen in the data but the long-term trends are well reproduced. Warming over the twentieth century is 0.7°C, in agreement with the IPCC estimate of 0.6° ± 0.2°C (Forster et al. 2007).

The simulated inventories of carbon in the atmosphere, ocean, and on land in the years 1800 and 1994 and their difference are given Table 1. The changes in carbon inventories over the historical period (1800–1994) compare relatively well with IPCC AR4 estimates (1750–1994). The observation-based changes in carbon reservoirs during the 1980s, 1990s, and 2000–05 are well reproduced by the model (Table 2). The atmospheric CO_2 increase is in close agreement with observations for the 1980s and 2000–05 but is overestimated in the 1990s. Ocean CO_2 uptake agrees very well with the observation-based values, but for a slight overestimation in 2000–05. Land CO_2 uptake falls well within the estimated uncertainty range for all time periods and is close to the IPCC best estimate.

The model reproduces qualitatively and quantitatively most features of the observation-based patterns of

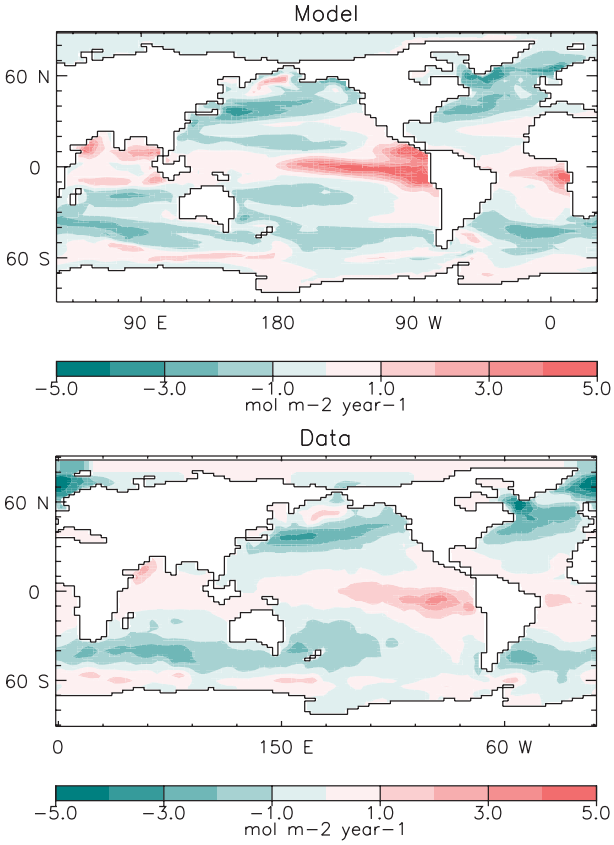

FIG. 2. Air–sea flux of carbon. (top) Model simulated fluxes at the year 2000 compared with (bottom) observational estimates (Takahashi et al. 2009). Negative values denote ocean uptake.

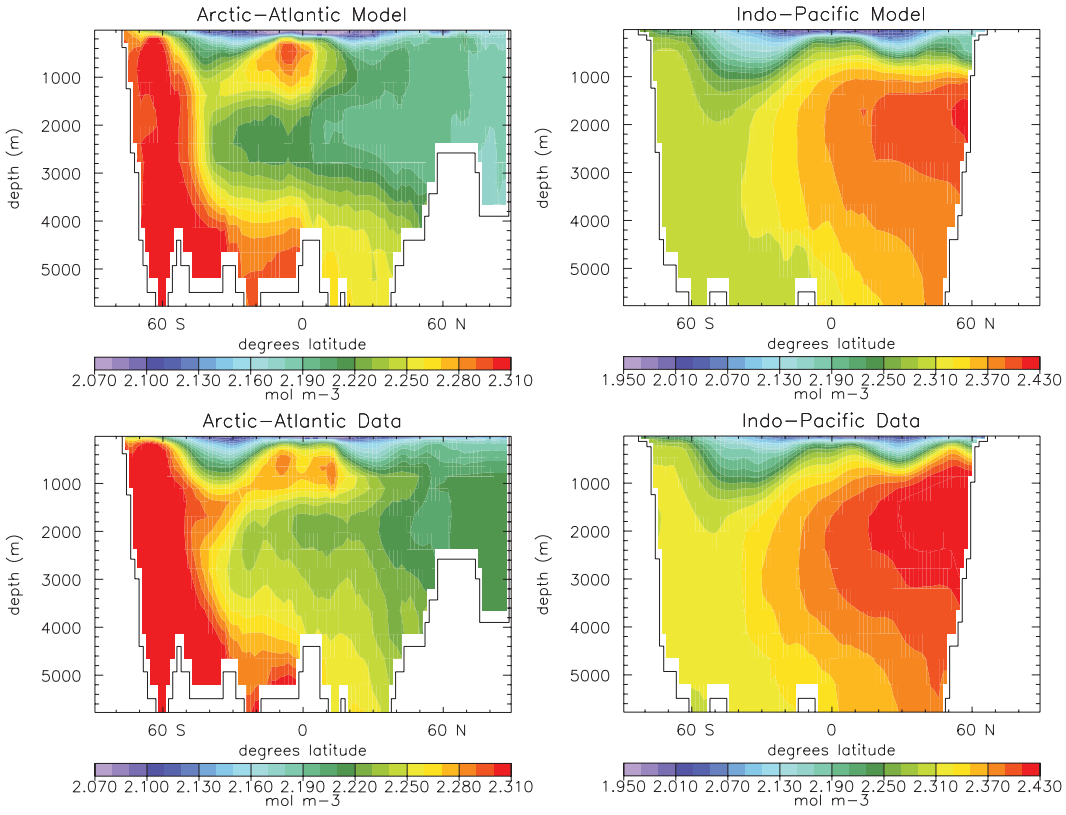

FIG. 3. (top) Model simulated zonally averaged DIC at the year 1994 compared with (bottom) GLODAP data (Key et al. 2004) for (left) Arctic–Atlantic and (right) Indo-Pacific oceans.

air–sea exchange of CO_2 (Fig. 2). These features include outgassing in low latitudes with a maximum in the eastern tropical Pacific and uptake at mid- and high latitudes with maxima around 40°N–S in the areas of the North Atlantic Current, the Kuroshio Current, and the Southern Ocean. Model biases include underestimated uptake in the Greenland–Iceland–Norwegian Seas and overestimated uptake in the eastern subtropical Pacific.

The simulated patterns of DIC and alkalinity show good agreement with observations (Figs. 3, 4). The model captures well the surface to deep gradient of both tracers. At depth the model slightly underestimates carbon while slightly overestimating alkalinity. See Table 3 for a summary of the average values and absolute errors of simulated DIC and alkalinity for the global, Arctic–Atlantic, and Indo-Pacific oceans. The simulated patterns of $CaCO_3$ are also in reasonable agreement with observations (Fig. 5). Nevertheless, the model underestimates deep $CaCO_3$ at tropical latitudes and overestimates $CaCO_3$ at high latitudes. Comparing only locations with observations, the global average percent of $CaCO_3$ in sediments is 34.5% for the data and 31.1% for the model.

3. Experimental design

The model was spun up for 10 000 yr with atmospheric carbon dioxide levels and Earth's orbital configuration specified for the year 1800 and the continental $CaCO_3$ weathering flux diagnosed from the ocean sediment burial flux. The weathering flux was then held fixed while the burial flux of $CaCO_3$ was allowed to evolve with time for all subsequent experiments. Historical emissions were applied until the end of the year 2000. These historical CO_2 emissions include contributions from both fossil fuel burning and land use changes. All other transient forcings (insolation, orbital forcing, tropospheric and stratospheric sulfates, and non-CO_2 greenhouse gases such as CH_4, N_2O, and CFCs) were held fixed.

At the beginning of 2001, "pulses" of CO_2 were applied over 1 yr. The emissions varied from 160 PgC (10^{15} g of carbon) to 5120 PgC (Table 4). The upper bound approximates all known conventional fossil fuel reserves (Rogner 1997). In addition to the pulse experiments, we also performed simulations with more "realistic" emissions scenarios. As a baseline, we assumed that emissions follow the A2 scenario up to the

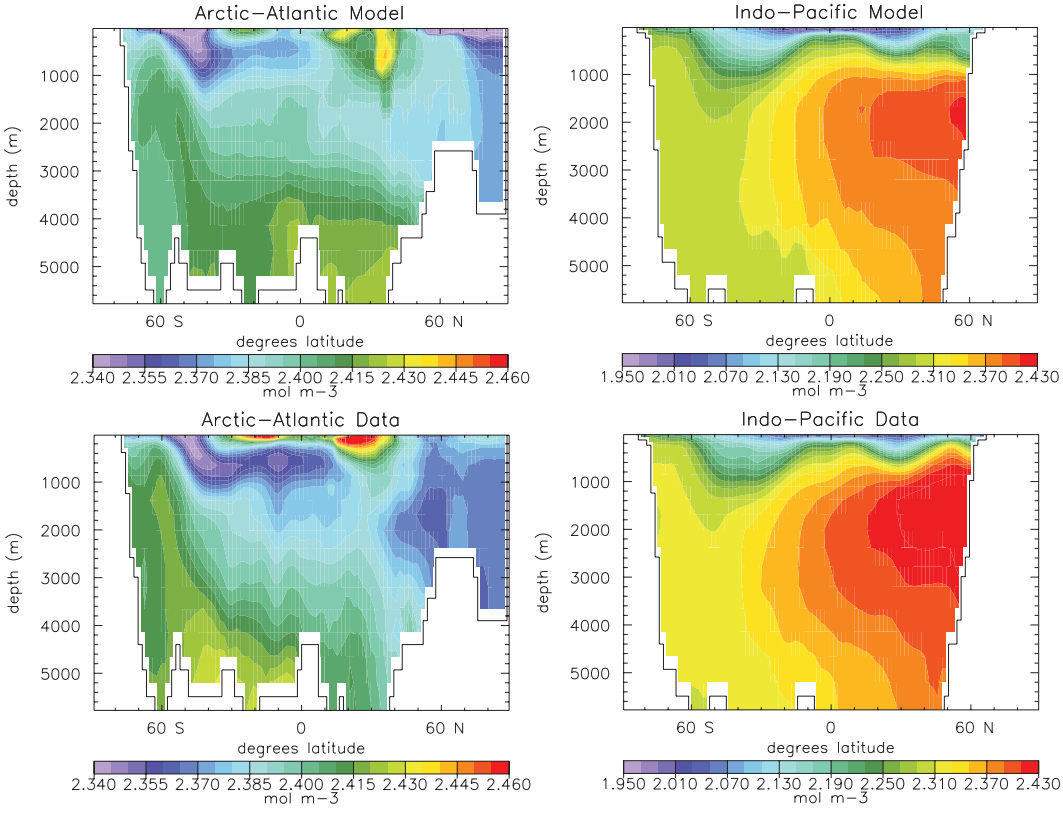

FIG. 4. (top) Model simulated zonally averaged alkalinity at the year 1994 compared with (bottom) GLODAP data (Key et al. 2004) for (left) Arctic–Atlantic and (right) Indo-Pacific oceans.

year 2100 and then decline linearly to zero by 2300. This scenario is designated as A2+ (Montenegro et al. 2007). We then generated a set of scenarios in which the A2+ emissions were scaled such that the cumulative emissions reached those of the equivalent pulse simulation by the year 2300. A2+ and pulse simulations were integrated for 5000 and 10 000 model years, respectively. To explore the consequences of future emissions only, a 10 000-yr control simulation was also carried out with zero emissions after the year 2000. At the end of this integration the SAT was again at its year 2000 value (having dropped 0.1°C from its temporary maximum) whereas CO_2 had dropped by 55 ppmv to 321 ppmv. These control results are subtracted from the results of the future emissions experiments.

4. Discussion and conclusions

Resulting maximum changes in atmospheric CO_2 range from 26 to 2352 ppmv (Fig. 6; Table 4). In the pulse experiments, the maximum CO_2 anomaly occurs at the beginning, initially decaying very rapidly but slowing after several decades. In the A2+ experiments, atmospheric CO_2 peaks a few decades before the year emissions are set to zero (260–286 yr; Table 4). After the peak, CO_2 closely approaches the level of the corresponding pulse experiment after about 500 yr. This demonstrates that the long-term atmospheric CO_2 response is nearly independent of the rate of CO_2 emissions (assuming all emissions occur over the next 300 yr).

TABLE 3. Model (M), data estimate (D; Key et al. 2004), and absolute error (E) for DIC and Alkalinity averaged over the Global, Arctic–Atlantic, and Indo-Pacific oceans for the year 1994.

	Global			Arctic–Atlantic			Indo-Pacific		
	M	D	E	M	D	E	M	D	E
DIC (mol m^{-3})	2.291	2.309	0.022	2.233	2.246	0.019	2.311	2.331	0.023
Alkalinity (mol m^{-3})	2.424	2.421	0.014	2.396	2.392	0.012	2.434	2.431	0.014

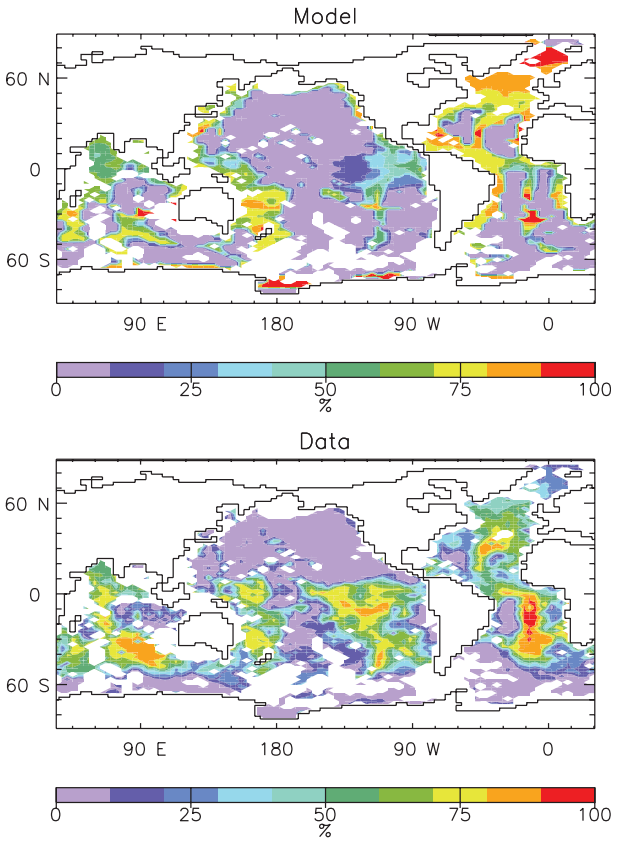

FIG. 5. (top) Model simulated percent dry weight $CaCO_3$ at year 2000 compared with (bottom) coretop data (Archer 1996b). Note that only locations with data are shown in both panels to facilitate the comparison.

A considerable amount (15%–30%) of the atmospheric CO_2 anomaly persists at the end of the 10 000-yr simulations (Fig. 6). The time to absorb a given percent of emissions is strongly dependent on the total amount of emissions (Fig. 7; Table 4). For emissions up to about 1000 PgC, 50% of the CO_2 anomaly is taken up within 100 yr and another 30% is absorbed within 1000 yr, which is similar to IPCC estimates (Denman et al. 2007). Above 1000 PgC, the time to absorb 50% of the emissions increases dramatically, and more than 2000 yr are needed to absorb half of a 5000-PgC perturbation.

Ocean surface pH is strongly coupled to atmospheric CO_2 (Caldeira and Wicket 2003). Emissions above 1280 PgC result in a decrease in average ocean surface pH that is larger than the 0.2 guard rail proposed by the German Advisory Council on Global Change (WGBU; Schubert et al. 2006; Fig. 8). Given the slow decay of atmospheric CO_2, experiments with emissions of 2560 PgC and larger still have lower pH than the 0.2 guard rail after 10 000 yr. For high emissions, the change in surface pH would probably have a significant impact on oceanic biota. Emissions of 1920 PgC and above result in minimum pH levels below 7.9, a value that could bring the aragonite saturation depth to the surface in the Southern Ocean generating serious adverse effects on calcifying organisms (Orr et al. 2005).

There is a lag in the response of surface air temperature to the CO_2 forcing (Fig. 9). For all but the lowest emissions, temperature reaches its maximum at least 550 yr after the peak in atmospheric CO_2 (Table 4). The lag is particularly pronounced in the experiments with

TABLE 4. Level and year of maximum CO_2 (Max CO_2), first year at which 50% of total emissions have been absorbed from the atmosphere (50% emissions), level and year of maximum SAT (Max SAT), and the first year at which SAT is less than 80% of the maximum (80% max SAT).

	Max CO_2			Max SAT		
Expt (Pg)	(ppmv)	(yr)	50% emissions (yr)	(°C)	(yr)	80% max SAT (yr)
160	69	1	18	0.32	247	527
160_A2+	26	270	187	0.32	342	1787
320	139	1	23	0.61	110	2230
640	280	1	36	1.38	3519	4363
640_A2+	118	260	201	1.40	3357	4153
960	423	1	63	2.00	2047	3126
1280	568	1	105	2.55	1965	3521
1280_A2+	274	269	232	2.53	2110	3583
1920	859	1	218	3.70	1147	3441
2560	1155	1	428	4.75	715	3929
2560_A2+	699	278	520	4.72	832	3943
3200	1453	1	781	5.66	809	4441
3840	1752	1	1309	6.48	1076	5066
3840_A2+	1223	284	1388	6.43	1147	4986
4480	2051	1	1732	7.24	1085	5248
5120	2352	1	2151	7.86	971	6190
5120_A2+	1781	286	2210	7.82	1287	>5000

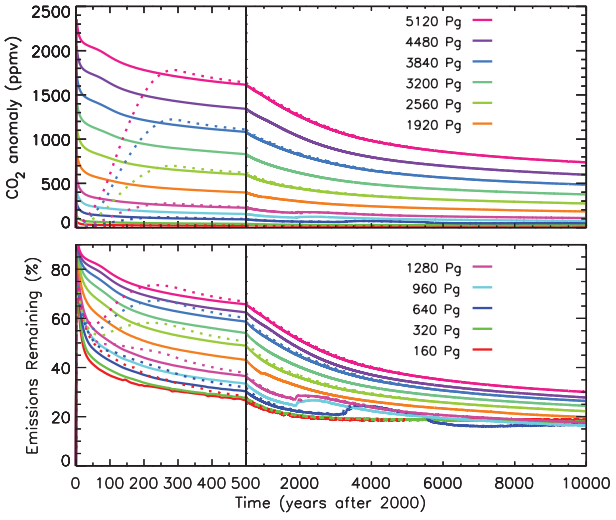

FIG. 6. Temporal changes in CO_2. Differences (top) relative to the control and (bottom) in terms of the percentage of CO_2 emissions remaining in the atmosphere. Note the different scales along the time axis. Colors indicate total emissions, with solid lines for pulse scenarios and dotted lines for equivalent A2+ scenarios.

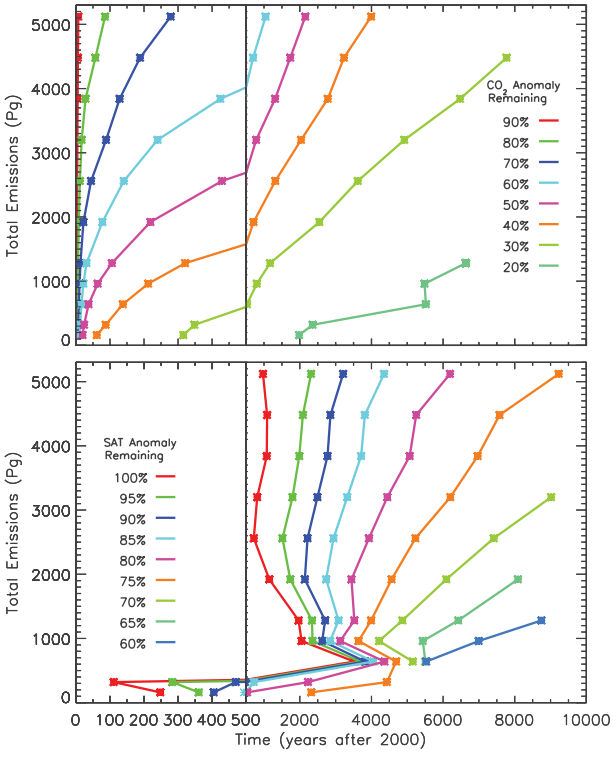

FIG. 7. Percentages of anomalies remaining: (top) CO_2 and (bottom) SAT. Stars indicate experimental points and lines are just visual aids. Note the different scales along the time axis and that colors indicate different percentages remaining, not total emissions, as in Figs. 6, 8, 9. For clarity, results for equivalent A2+ scenarios are not shown. The SAT anomaly is noisy for low emissions due to long time-scale climate variability (see Fig. 9 and text).

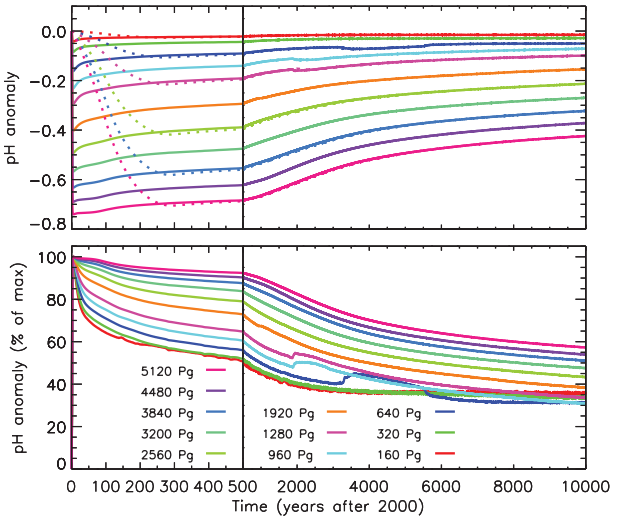

FIG. 8. Temporal changes in sea surface pH. (top) Differences relative to the control simulation and (bottom) differences in terms of the percentage of the maximum pH anomaly remaining. Note the different scales along the time axis. Colors indicate total emissions, with solid lines for pulse scenarios and dotted lines for equivalent A2+ scenarios. Results for equivalent A2+ scenarios are not shown in the bottom panel for clarity.

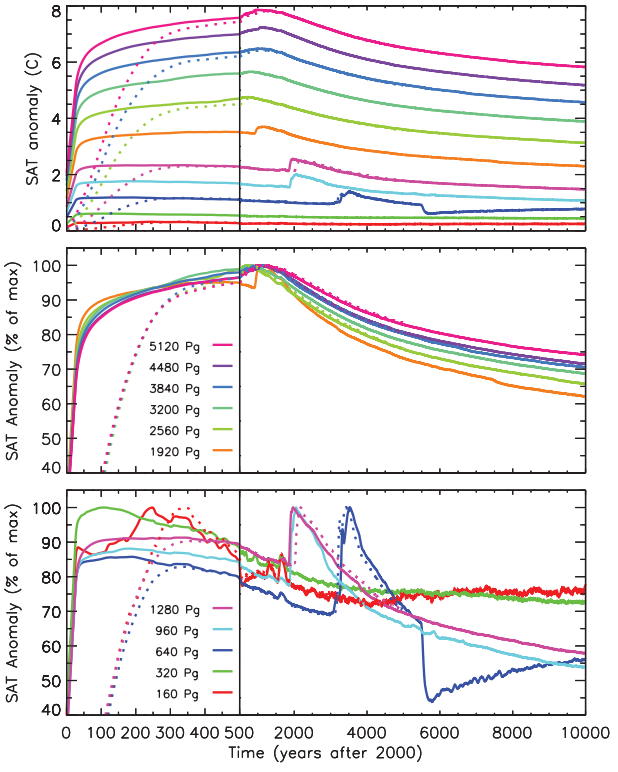

FIG. 9. Temporal changes in SAT. Differences (top) relative to the control and as a percentage of the maximum SAT anomaly for (middle) high and (bottom) low emissions. High and low emissions are plotted separately for clarity. Note the different scales along the time axis. Colors indicate total emissions, with solid lines for pulse scenarios and dotted lines for equivalent A2+ scenarios.

total emissions in the range 640–1280 PgC, where after 2000–3500 yr, the planetary cooling is suddenly reversed and SAT again increases by as much as 0.5°C. This abrupt warming and accompanying increase in CO_2 is caused by flushing events in the Southern Ocean, which in this model have been shown to be dependent on the level of atmospheric CO_2 (Meissner et al. 2008). Under the A2+ emissions scenarios, the peak in SAT is almost identical to the corresponding pulse experiments, indicating that the long-term temperature response is independent of the rate of CO_2 emissions (Fig. 9; Table 4).

The SAT anomaly is even longer lived than the CO_2 anomaly. For all experiments, at least 50% of the maximum temperature anomaly persists at the end of the simulation. For both the smallest and largest emission scenarios, the temperature anomaly remaining after 10 000 yr is about 75% of the maximum anomaly. Similar to CO_2, the time to reduce temperature by a specific percent of the maximum anomaly depends on the total amount of emissions. The time within which SAT declines by 20% relative to the peak warming ranges from about 500 yr for the lowest emission scenario to more than 5000 yr for the highest emissions scenarios (Fig. 7; Table 4).

Given that the change in temperature from preindustrial to the year 2000 is about 0.8°C (Fig. 1), total emissions of 640 PgC or more result in average air temperatures above the 2°C temperature guard rail suggested by the WBGU (Schubert et al. 2006) and endorsed by the European Union. The threshold to stay below this guard rail would appear to be near 640 PgC of total emissions from the year 2000. Experiments with emissions of 1280 PgC and larger still exceed the 2°C guard rail after 10 000 yr.

To estimate the perturbation lifetime of anthropogenic climate change the response curves of either CO_2 or temperature were fit to an exponential formula of the form $A_0\exp(-t/A_1) + A_2$. The parameter A_0 gives an estimate of the amount a quantity is reduced, A_1 is the average lifetime, and A_2 is the amount of any very long-lived residual. We restrict our analysis to experiments with total emissions greater than 1500 PgC. In simulations with lower emissions, the response curve is often contaminated by noise, making curve fitting imprecise (Figs. 6, 9).

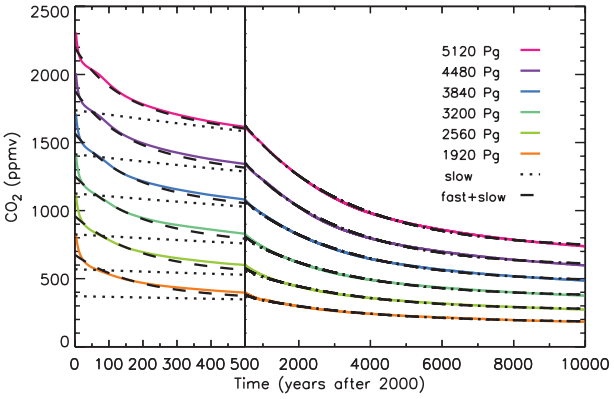

FIG. 10. Curve fitting to a double exponential model. Dotted lines are an exponential fit to simulated CO_2 after 1000 yr and are used to estimate the slow time scale for reducing CO_2 (slow). These curves were extrapolated back 1000 yr and the extrapolated CO_2 was subtracted from the simulated CO_2. A second exponential fit was performed on the remaining CO_2 to estimate a fast time scale for reducing CO_2 (fast). The dashed curves are the sum of two exponential curves (fast + slow). Note the different scales along the time axis.

A gradient-expansion algorithm was used to compute the least squares fit of an exponential model to the data. To tease out a fast and slow time scale for uptake of CO_2, an exponential fit was first applied to the CO_2 curves after 1000 yr. The data fit an exponential very well (see Fig. 10). This curve was then extrapolated back 1000 yr and the extrapolated CO_2 was subtracted from the simulated CO_2. A second exponential fit was performed on the remaining CO_2. This fit is clearly not as good as the previous fit (Fig. 10). The early response is not a pure exponential but a combination of processes with different time scales (Joos et al. 1996). Still, this analysis

TABLE 5. Average perturbation lifetimes in years and percentages reduced. The average perturbation lifetimes are calculated from exponential fits to model results. Percentages are of either total CO_2 emissions or maximum SAT. All are calculated from differences with the control (control has zero emissions from year 2001 onward).

	CO_2					SAT		
	Fast		Slow			Slow		
Expt (Pg)	(years)	(%)	(yr)	(%)	$\gg$10 000 yr (%)	(yr)	(%)	$\gg$10 000 yr (%)
1920	146	56	3000	24	20	3400	39	61
2560	149	50	3000	28	22	3900	37	63
3200	136	43	2700	33	24	3900	34	66
3840	129	36	2900	38	26	4300	34	66
4480	102	29	2600	43	28	4100	31	69
5120	107	27	2900	44	29	4600	31	69

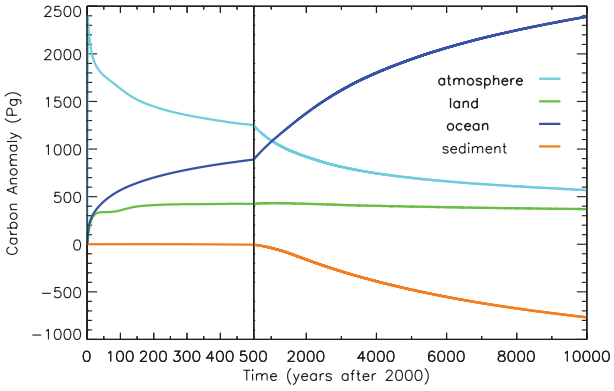

FIG. 11. Temporal changes in carbon pools. Differences in carbon relative to the control simulation for the 2560-PgC pulse experiment. The sediment pool includes changes due to continental weathering. Note the different scales along the time axis.

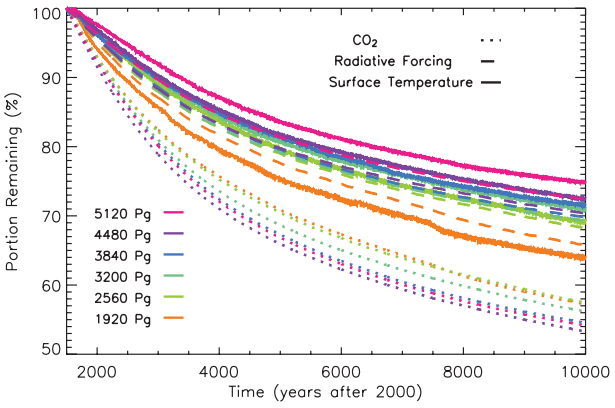

FIG. 12. Portion of anomalous CO_2, radiative forcing, and surface temperature relative to 1500 yr after the start of the simulation. Although sometimes indistinct in the figure, the radiative forcing and temperature curves are similar: both show longer time scales (decline less steeply) than CO_2 and time scales become longer as emissions increase.

provides a reasonable, if somewhat uncertain, estimate of the overall fast absorption time scale. Although the estimated short-term-response time scale may be dependent on the number of exponentials used in the fit (Maier-Reimer and Hasselmann 1987), the longer response time scale (after 1000 yr) is quite robust and reasonably independent of the section of the curve used in the fit. The perturbation lifetime of CO_2 is thus broken up into a period of rapid absorption, a period of slow absorption, and a "residual" that represents CO_2, which stays in the atmosphere for longer than this method can resolve ($\gg$10 000 yr). To derive a perturbation lifetime for temperature, we also fit an exponential model to the temperature response curves after the year 1000.

We find that the response curves for CO_2 can be well approximated by the superposition of exponentials with two different time scales. The average lifetime for the short time scale is about 130 yr whereas the long time scale has an average lifetime closer to 2900 yr (Table 5). The amount of CO_2 absorbed by processes associated with the short time-scale sink are nearly constant (1075–1382 PgC; calculated from Table 5). About 400 PgC of the short time-scale sink is associated with increased land uptake (mostly through CO_2 fertilization), whereas the rest (~900 PgC) are due to relatively rapid dissolution in the surface ocean (Fig. 11). The longer time scale of the deep-ocean sink is associated with slow rates of deep-ocean transport and carbonate dissolution. The amount taken up by the deep-ocean sink is not constant but increases at higher levels of emissions, implying that the sink is not saturated. The absorption time scale for CO_2 does not seem to be very sensitive to the amount of emissions (Table 5).

For high-emission experiments, after year 1000 (roughly the year of maximum temperature), a single exponential fits the temperature response very well. The average perturbation lifetime is about 4000 yr, or 40% longer than the average for CO_2. The temperature perturbation lifetime also appears to be more dependent on the level of total emissions than the CO_2 perturbation lifetime (Table 4).

Radiative forcing from atmospheric CO_2 depends on the logarithm of CO_2, but for the first 1000 yr, the thermal inertia of the ocean and climate feedbacks are important in keeping SAT below what would be expected from the radiative forcing alone (Meehl et al. 2007). After 1000 yr, the time scale for reducing SAT becomes very similar to the time scale of the CO_2 radiative forcing and this time scale is considerably longer than for CO_2. The logarithmic dependence of the radiative forcing on CO_2 is also why the SAT perturbation lifetime depends on the total amount of emissions, even though the time scale of CO_2 absorption itself appears to be relatively constant.

Figure 12 shows the portion of CO_2, radiative forcing from CO_2, and surface temperature normalized to their values at 1500 yr. The spread in the time scales for CO_2 (illustrated by the spread in the curves) is relatively small and larger emissions seem to show slightly shorter time scales (steeper slopes) than smaller emissions (also see Table 5). Radiative-forcing time scales are longer than for CO_2 alone and, as with temperature, the time scale for the decay of the radiative forcing increases as emissions increase. The temperature time-scale dependency on emissions can mostly be explained by the changes in radiative-forcing time scales, although other feedbacks make the spread in temperature time scales even larger.

In summary, this study suggests that for emissions less than about 1500 PgC, most of the CO_2 will be absorbed within a few centuries, which is in agreement with earlier work. Temperature anomalies may last much longer. With larger emissions, the time to absorb most of the CO_2 increases rapidly (Table 4; Fig. 7). This dependency of the CO_2 response on the level of emissions has important policy implications and needs to be investigated with other models. A long-term model intercomparison project (LTMIP) with standardized experiments has recently been initiated and this will hopefully further increase our understanding and reduce the uncertainty in the long-term carbon cycle response. Preliminary results from nine models (including the one used here) can be found in Archer et al. (2009).

Although the long-term climate–carbon cycle response still remains highly uncertain, the model used in this study suggests that for large emissions, the perturbation lifetime of both CO_2 and surface temperature might be longer than previously thought. The long-term climate response appears to be independent of the rate at which CO_2 is emitted over the next few centuries. Regardless of the future emissions trajectory, changes to the earth's climate will likely persist for several thousands of years. The logarithmic relationship between CO_2 and its radiative forcing implies that the time scale at which atmospheric temperature declines will be longer than the time scale of CO_2. For ecosystems having already adapted to a warmer world, slow cooling may be beneficial. Nevertheless, it is sobering to ponder the notion that the carbon we emit over a handful of human lifetimes may significantly affect the earth's climate over tens of thousands of years.

REFERENCES

Archer, D., 1996a: A data-driven model of the global calcite lysocline. *Global Biogeochem. Cycles,* **10,** 511–526.

——, 1996b: An atlas of the distribution of calcium carbonate in sediments of the deep sea. *Global Biogeochem. Cycles,* **10,** 159–174.

——, 2005: Fate of fossil fuel CO_2 in geologic time. *J. Geophys. Res.,* **110,** C09S05, doi:10.1029/2004JC002625.

——, and V. Brovkin, 2008: The millennial atmospheric lifetime of anthropogenic CO_2. *Climatic Change,* **90,** 283–297, doi:10.1007/s10584-008-9413-1.

——, H. Kheshgi, and E. Maier-Reimer, 1998: Dynamics of fossil fuel CO_2 neutralization by marine $CaCO_3$. *Global Biogeochem. Cycles,* **12,** 259–276.

——, and Coauthors, 2009: Atmospheric lifetime of fossil-fuel carbon dioxide. *Annu. Rev. Earth Planet. Sci.,* **37,** 117–134.

Caldeira, K., and M. E. Wickett, 2003: Anthropogenic carbon and ocean pH. *Nature,* **425,** 365.

Denman, K. L., and Coauthors, 2007: Couplings between changes in the climate system and biogeochemistry. *Climate Change 2007: The Physical Science Basis*, S. Solomon et al., Eds., Cambridge University Press, 589–662.

Etheridge, D. M., L. P. Steele, R. L. Langenfelds, R. J. Francey, J.-M. Barnola, and V. I. Morgan, 1998: Historical CO_2 records from the Law Dome DE08, DE08-2, and DSS ice cores. *Trends: A Compendium of Data on Global Change,* Carbon Dioxide Information Analysis Center. [Available online at http://cdiac.esd.ornl.gov/trends/co2/lawdome.html.]

Forster, P., and Coauthors, 2007: Changes in atmospheric constituents and in radiative forcing. *Climate Change 2007: The Physical Science Basis,* S. Solomon et al., Eds., Cambridge University Press, 129–234.

Friedlingstein, P., and Coauthors, 2006: Climate–carbon cycle feedback analysis: Results from the C^4MIP model intercomparison. *J. Climate,* **19,** 3337–3353.

Gent, P. R., and J. C. McWilliams, 1990: Isopycnal mixing in ocean circulation models. *J. Phys. Oceanogr.,* **20,** 150–155.

Gregory, J. M., and Coauthors, 2005: A model intercomparison of changes in the Atlantic thermohaline circulation in response to increasing atmospheric CO_2 concentration. *Geophys. Res. Lett.,* **32,** L12703, doi:10.1029/2005GL023209.

Jones, P. D., D. E. Parker, T. J. Osborn, and K. R. Briffa, 2008: Global and hemispheric temperature anomalies—Land and marine instrumental records. *Trends: A Compendium of Data on Global Change,* Carbon Dioxide Information Analysis Center. [Available online at http://cdiac.ornl.gov/trends/temp/jonescru/jones.html.]

Joos, F., M. Bruno, R. Fink, U. Siegenthaler, T. F. Stocker, and C. LeQuere, 1996: An efficient and accurate representation of complex oceanic and biospheric models of anthropogenic carbon uptake. *Tellus,* **48B,** 397–417.

Keeling, C. D., and T. P. Whorf, 2005: Atmospheric CO_2 records from sites in the SIO air sampling network. *Trends: A Compendium of Data on Global Change,* Carbon Dioxide Information Analysis Center. [Available online at http://cdiac.ornl.gov/trends/co2/sio-keel.html.]

Key, R. M., and Coauthors, 2004: A global ocean carbon climatology: Results from Global Data Analysis Project (GLODAP). *Global Biogeochem. Cycles,* **18,** GB4031, doi:10.1029/2004GB002247.

Lenton, T. M., and C. Britton, 2006: Enhanced carbonate and silicate weathering accelerates recovery from fossil fuel CO_2 perturbations. *Global Biogeochem. Cycles,* **20,** GB3009, doi:10.1029/2005GB002678.

——, and Coauthors, 2006: Millennial timescale carbon cycle and climate change in an efficient Earth system model. *Climate Dyn.,* **26,** 687–711.

Maier-Reimer, E., and K. Hasselmann, 1987: Transport and storage of CO_2 in the ocean—An inorganic ocean-circulation carbon cycle model. *Climate Dyn.,* **2,** 63–90.

Matthews, H. D., A. J. Weaver, K. J. Meissner, N. P. Gillett, and M. Eby, 2004: Natural and anthropogenic climate change: Incorporating historical land cover change, vegetation dynamics and the global carbon cycle. *Climate Dyn.,* **22,** 461–479.

Meehl, G. A., and Coauthors, 2007: Global climate projections. *Climate Change 2007: The Physical Science Basis,* S. Solomon et al., Eds., Cambridge University Press, 747–845.

Meissner, K. J., A. J. Weaver, H. D. Matthews, and P. M. Cox, 2003: The role of land surface dynamics in glacial inception: A study with the UVic Earth System model. *Climate Dyn.,* **21,** 515–537.

——, M. Eby, A. J. Weaver, and O. A. Saenko, 2008: CO_2 threshold for millennial-scale oscillations in the climate system: Implications for global warming scenarios. *Climate Dyn.,* **30,** 161–174.

Mikolajewicz, U., M. Gröger, E. Maier-Reimer, G. Schurgers, M. Vizcaíno, and A. M. E. Winguth, 2007: Long-term effects of anthropogenic CO_2 emissions simulated with a complex earth system model. *Climate Dyn.,* **28,** 599–633.

Montenegro, A., V. Brovkin, M. Eby, D. Archer, and A. J. Weaver, 2007: Long term fate of anthropogenic carbon. *Geophys. Res. Lett.,* **34,** L19707, doi:10.1029/2007GL030905.

Orr, J. C., and Coauthors, 2005: Anthropogenic ocean acidification over the twenty-first century and its impacts on calcifying organisms. *Nature,* **437,** 681–686.

Plattner, G.-K., and Coauthors, 2008: Long-term climate commitments projected with climate–carbon cycle models. *J. Climate,* **21,** 2721–2751.

Ridgwell, A., and J. C. Hargreaves, 2007: Regulation of atmospheric CO_2 by deep-sea sediments in an Earth system model. *Global Biogeochem. Cycles,* **21,** GB2008, doi:10.1029/2006GB002764.

——, I. Zondervan, J. C. Hargreaves, J. Bijma, and T. M. Lenton, 2007: Assessing the potential long-term increase of oceanic fossil fuel CO_2 uptake due to CO_2-calcification feedback. *Biogeosciences,* **4,** 481–492.

Rogner, H. H., 1997: An assessment of world hydrocarbon resources. *Annu. Rev. Energy Environ.,* **22,** 217–262.

Sarmiento, J. L., and N. Gruber, 2006: *Ocean Biogeochemical Dynamics*. Princeton University Press, 526 pp.

Schmittner, A., A. Oschlies, H. D. Matthews, and E. D. Galbraith, 2008: Future changes in climate, ocean circulation, ecosystems and biogeochemical cycling simulated for a business-as-usual CO_2 emission scenario until year 4000 AD. *Global Biogeochem. Cycles,* **22,** GB1013, doi:10.1029/2007GB002953.

Schubert, R., and Coauthors, 2006: The future oceans—Warming up, rising high, turning sour. Wissenschaftlicher Beirat der Bundesregierung Globale Umweltveränderungen Special Rep., 110 pp.

Stouffer, R. J., and Coauthors, 2006: Investigating the causes of the response of the thermohaline circulation to past and future climate changes. *J. Climate,* **19,** 1365–1387.

Takahashi, T., and Coauthors, 2009: Climatological mean and decadal changes in surface ocean pCO_2, and net sea-air CO_2 flux over the global oceans. *Deep-Sea Res. II,* in press.

Tyrrell, T., J. G. Shepherd, and S. Castle, 2007: The long-term legacy of fossil fuels. *Tellus,* **59B,** 664–672.

Weaver, A. J., and Coauthors, 2001: The UVic Earth System Climate Model: Model description, climatology, and applications to past, present and future climates. *Atmos.–Ocean,* **39,** 361–428.

——, M. Eby, M. Kienast, and O. A. Saenko, 2007: Response of the Atlantic meridional overturning circulation to increasing atmospheric CO_2: Sensitivity to mean climate state. *Geophys. Res. Lett.,* **34,** L05708, doi:10.1029/2006GL028756.

Weber, S. L., and Coauthors, 2007: The modern and glacial overturning circulation in the Atlantic Ocean in PMIP coupled model simulations. *Climate Past,* **3,** 51–64.